Charge effects on hindrance factors for diffusion and convection of solute in pores I

Hideyuki O-tani[1], Takeshi Akinaga[2] and Masako Sugihara-Seki[2]

[1]Graduate School of Science and Engineering, Kansai University, Yamate-cho, Suita, Osaka, 564-8680, JAPAN

[2]Department of Pure and Applied Physics, Kansai University, Yamate-cho, Suita, Osaka, 564-8680, JAPAN

E-mail: ga8d002@kansai-u.ac.jp

Abstract. The transport of a spherical solute through a long circular cylindrical pore filled with an electrolyte solution is studied numerically, in the presence of constant surface charge on the solute and the pore wall. Fluid dynamic analyses were carried out to calculate the flow field around the solute in the pore to evaluate the drag coefficients exerted on the solute. Electrical potentials around the solute in the electrolyte solution were computed based on a mean-field theory to provide the interaction energy between the charged solute and pore wall. Combining the results of the fluid dynamic and electrostatic analyses, we estimated the rate of the diffusive and convective transport of the solute across the pore. Although the present estimates of the drag coefficients on the solute suggest more than 10% difference from existing studies, depending on the radius ratio of the solute relative to the pore and the radial position of the solute center in the pore, this difference leads to a minor effect on the hindrance factors. It was found that even at rather large ion concentrations, the repulsive electrostatic interaction between the solute and the pore wall of like charge could significantly reduce the transport rate of the solute.

Keywords: Hindrance factors, Electrical Charge Effect, Pore theory

1. Introduction

The transport of solute molecules through porous membranes has been investigated extensively in engineering and biological applications, such as microvascular permeability, glomerular filtration, sieving of macromolecules by artificial porous membranes and so on. When the solute has a dimension comparable to the size of the pores, the rate of solute transport tends to be lower than in bulk solution. This phenomenon, termed hindered transport, can be explained largely by a combination of steric and hydrodynamic interaction between the permeating solute and the pore wall. If the solute and the pore wall are electrically charged, then the electrostatic interaction between them could affect the rate of the hindered transport. In fact, significant contributions of electric charge to the microvascular permeability have been reported for capillaries in various tissues (Curry 1984). In the present study, we examine the electrostatic effect on the hindered transport of charged spherical solutes through charged circular cylindrical pores, by combining fluid dynamic and electrostatic analyses.

When the radius of the pore and that of the solute molecule greatly exceed that of solvent molecules, the solute can be treated as a particle and the solvent as a continuum. Under this condition, Deen (1987) reviewed the hydrodynamic theory for the hindered transport of solute across porous membranes. He considered a membrane with circular cylindrical pores of radius r_c and length L, separating two reservoirs of solute concentrations c_0 and c_L. For a spherical solute of radius a, the solute flux averaged over the pore cross-section $\langle N \rangle$ is expressed in terms of the solvent average velocity V and a potential energy of interaction between the solute and the pore wall E (Deen 1987):

$$\langle N \rangle = WVc_0 \frac{1-(c_L/c_0)e^{-P_e}}{1-e^{-P_e}}, \tag{1}$$

$$P_e = \frac{WVL}{HD_\infty}, \tag{2}$$

$$H = 2\int_0^{1-a/r_\mathrm{c}} \frac{1}{F_\mathrm{t}(\beta)} e^{-E(\beta)/kT} \beta d\beta, \tag{3}$$

$$W = 2\int_0^{1-a/r_\mathrm{c}} \frac{F_0(\beta)}{F_\mathrm{t}(\beta)} e^{-E(\beta)/kT} \beta d\beta, \tag{4}$$

where D_∞ represents the diffusivity of the solute in dilute bulk solution, k is the Boltzmann constant and T is the absolute temperature. The dimensionless variable β represents the radial position of the solute center relative to the pore radius. The coefficients F_t and F_0 represent hydrodynamic drag coefficients defined as $F_\mathrm{t} = F/6\pi\mu aU$ and $F_0 = F'/6\pi\mu aV$, where F is the hydrodynamic force acting on a solute translating parallel to the pore axis at velocity U in an otherwise quiescent fluid with viscosity μ, and F' is the force exerted on a stationary solute immersed in a Poiseuille flow through the pore with mean velocity V. The potential energy $E(\beta)$ describes the interaction between the solute and the pore wall, such as steric restriction and electrostatic interaction when the solute center is placed at a radial

position β in the pore. If only steric restriction is present in uncharged cases, $E(\beta) = 0$ for $0 \leq \beta < 1 - a/r_c$ and $E(\beta) = \infty$ for $1 - a/r_c \leq \beta \leq 1$. Note that the so-called Boltzmann factor $\exp(-E(\beta)/kT)$ appeared in equations (3) and (4) reflects the probability of finding a solute at a given radial position β in the pore.

Equation (2) defines the Peclet number based on the pore length. The limiting forms of equation (1) for extremes of the Peclet number are

$$\langle N \rangle = \frac{HD_\infty}{L}(c_0 - c_L) \qquad \text{for} \quad P_e \ll 1, \tag{5}$$

$$\langle N \rangle = WVc_0 \qquad \text{for} \quad P_e \gg 1. \tag{6}$$

These expressions imply that the solute transport is dominated by diffusion for $P_e \ll 1$ and by convection for $P_e \gg 1$, and H and W are related to the rate of the diffusive transport and the convective transport of the solute, respectively. Since $H = W = 1$ in the case of $a \ll r_c$ or in an unbounded fluid, these are called hindrance factors. From equations (5) and (6), Deen (1987) indicated a relationship between the hindered transport theory and phenomenological transport coefficients for porous membranes. The solute permeability, which can be measured as the proportional constant of the solute flux per membrane area to the solute concentration difference (Curry 1984), is given by $\gamma HD_\infty/L$, where γ is the fraction of the membrane surface occupied by pores. The reflection coefficient, the fraction of solute rejected by the membrane, is given by $1 - W$.

In the presence of only steric restriction, Sugihara-Seki (2004) estimated F_t and F_0 for a spherical solute in a circular cylindrical pore, including the cases where the solvent is a Brinkman medium, and evaluated the solute permeability and the reflection coefficient. Dechadilok and Deen (2006) provided estimates of the hindrance factors H and W from equations (3) and (4), by adopting the values of F_t and F_0 reported by Higdon and Muldowney (1995). Higdon and Muldowney (1995) expressed F_t and F_0 as functions of the radial position of the solute center for the size ratios $a/r_c = 0.05$, 0.1, 0.2, ..., 0.9. Although their results of F_t and F_0 are in excellent agreement with those of Sugihara-Seki (2004) for $a/r_c = 0.3$, some discrepancy appears for $a/r_c = 0.7$, especially at off-center positions of the solute.

The electrostatic interaction between charged solute and pore wall has been studied for many years. Smith and Deen (1980) developed a model of electrostatic double-layer interaction between a spherical solute and a circular cylindrical pore, to evaluate its contributions to the potential energy of interaction $E(\beta)$. Since their analysis was limited to axisymmetric positions of the solute and therefore yielded only $E(0)$, they extended their analysis to include off-axis positions of the solute in the subsequent study (Smith and Deen 1983). Smith and Deen (1980, 1983) obtained analytical expressions for $E(\beta)$, and calculated equilibrium partitioning of solutes between pores and bulk solution, defined by

$$\Phi = 2\int_0^{1-a/r_c} e^{-E(\beta)/kT}\beta d\beta. \tag{7}$$

Quite recently, Dechadilok and Deen (2009) adopted approximate expressions of $E(\beta)$ to

estimate the value of H from equation (3), by taking the electric double-layer distortion into account. They showed that the repulsive electrostatic interaction between the solute and pore charge could significantly enlarge the hindered effect on the solute diffusion in pores.

In a previous study (Akinaga *et al* 2008), we have obtained by a numerical computation the interaction energy $E(\beta)$ for a charged solute in a charged cylindrical pore. Using the values of $E(\beta)$, we examined the effect of electrostatic interactions on the osmotic flow across membranes with circular cylindrical pores. Although Akinaga et al. (2008) employed the Poisson-Boltzmann equation to obtain the electrical potential and Smith and Deen (1980) adopted its linearized form, i.e. the Debye-Hückel equation, our obtained values of $E(0)$ for various values of size ratio a/r_c agree fairly well with the corresponding values in Smith and Deen (1980). For off-axis cases, the $E(\beta)$ values of our study agree with those of Smith and Deen (1983) to some extent except for the cases of large β, small ion concentrations and large charge densities.

In the work reported here, we computed the hydrodynamic coefficients F_t and F_0 as well as the interaction energy $E(\beta)$ based on the Debye-Hückel equation, and estimated the hindrance factors H and W from equations (3) and (4). The charge on the solute is taken to be of the same sign as that on the pore wall. Since Dechadilok and Deen (2009) showed that the effect of the double-layer distortion on the permeability is negligible for repulsive electrostatic interactions, we do not consider the distortion of the double layer in the current study. By estimating the values of H and W as functions of size ratio a/r_c, surface charge densities, and ion concentrations in the solvent, we examine the electrostatic effect on the hindered transport of charged spherical solutes through charged circular cylindrical pores.

2. Formulation and methods

We consider transport of spherical solutes of radius a across a porous membrane with circular cylindrical pores of radius r_c and length L ($r_\mathrm{c} \ll L$), as shown in figure 1. The membrane is placed between two solutions with different solute concentrations, c_0 and c_L ($c_0 > c_L$). The solute and the pore wall have uniform constant surface charge of density q_s and q_c, respectively, and the solvent is an electrolyte solution containing small cation and anion which can be regarded as point charge. We consider the case where q_s and q_c are of like charge and the electrolytes are univalent-univalent. We denote the ion concentration in the bulk solution as C_0 and assume $T = 310$ K. The pore is assumed to be long compared to its radius, so that the end effects of the pore can be neglected. It is also assumed that the solute volume fraction is small, implying that the mutual interaction between the solutes can be neglected.

2.1. Estimate of the interaction energy

The procedures to obtain the interaction energy, or excess free energy, between the solute and the pore wall were described in Akinaga *et al* (2008) and Sugihara-Seki *et al* (2010). Briefly, we adopted a mean-field theory and the electrical potential ψ around the solute placed in the pore was described by the Poisson-Boltzmann equation. In the limit of small ψ, the Poisson-Boltzmann equation can be reduced to the so-called Debye-Hückel equation:

$$\nabla^2\psi = \frac{1}{\lambda_{\mathrm{D}}^2}\psi, \tag{8}$$

where $\lambda_{\mathrm{D}} = \sqrt{\varepsilon RT/2F^2C_0}$ is the Debye length, defined for a univalent-univalent electrolyte. Here, ε is the solvent dielectric permittivity, R is the gas constant and F is the Faraday constant. In the present study, we solved equation (8) for a solute placed at arbitrary radial positions in the pore, subject to the boundary conditions:

$$\begin{aligned} &\varepsilon\partial_{\mathrm{n}}\psi = -q_{\mathrm{c}} \quad \text{on the surface of the pore,} \\ &\varepsilon\partial_{\mathrm{n}}\psi = -q_{\mathrm{s}} \quad \text{on the surface of the solute.} \end{aligned} \tag{9}$$

where ∂_{n} represents the derivative normal to the surface in the solvent region. We have assumed that the dielectric constants of the membrane material and the solute can be neglected compared to that of the solvent (Smith and Deen 1980). In the numerical computation, we employed a spectral element method to obtain the electrical potential (Akinaga et al. 2008, Sugihara-Seki et al. 2010). By the use of the electrical potential ψ, we defined the electrostatic energy in the field at a constant charge density q on the surface ∂V (Smith and Deen 1980):

$$U = \int_{\partial V} dA \int_0^q \psi dq. \tag{10}$$

The interaction energy E was obtained as the difference between the electrostatic energy of the solute-pore system and that of the individual solute and pore at infinite separation, i.e.

$$E = U_{\mathrm{CS}} - U_{\mathrm{C}} - U_{\mathrm{S}}, \tag{11}$$

where the subscript CS designates the case in which both solute and pore wall are electrically charged, the subscript C denotes the case in which only charged pore is present, and the subscript S denotes the case in which only charged solute is present (Akinaga *et al* 2008).

2.2. Estimate of F_{t} and F_0

As mentioned above, the coefficients F_{t} and F_0 in equations (3) and (4) represent the drag coefficients for a spherical solute translating parallel to the pore axis in an otherwise quiescent fluid or a stationary solute immersed in a Poiseuille flow. Since the Reynolds number is extremely small in the cases considered, we solved the Stokes equation and the continuity equation to obtain the flow field around the solute placed at arbitrary

radial positions in the circular cylindrical pore. In the numerical computation, we employed a hp-finite element method (O-tani and Sugihara-Seki 2010, Schawab 1998). The numerical accuracy of the method was examined closely in O-tani and Sugihara-Seki (2010). From the velocity field obtained, we computed the hydrodynamic forces exerted on the solute to estimate F_t and F_0 as functions of the radial position of the solute center β and the size ratio a/r_c. In the current study, we did not include electrostatic effects on the flow field, which is related to the distortion of the double layer.

2.3. Estimate of H and W

The obtained values of E as well as F_t and F_0 were inserted into equations (3) and (4) to compute the values of H and W. The hindrance factors H and W were expressed as functions of the charge densities q_s, q_c, the ion concentration C_0, and the size ratio a/r_c for prescribed pore radius r_c. The numerical integrations in equations (3) and (4) were performed by employing the Gauss-Lobatto-Legendre formulae of the 10th degree.

3. Results

Even for purely steric case, i.e. $E(\beta) = 0$ for $0 \leq \beta < 1 - a/r_c$, it is quite recently that the dependences of F_t and F_0 on β are included in the estimate of H and W (Sugihara-Seki 2004, Dechadilok and Deen 2006). Sugihara-Seki (2004) computed the values of F_t and F_0 by a finite element method and Dechadilok and Deen (2006) adopted them from Higdon and Muldowney (1995). Before them, most theoretical studies assumed centerline approximation such that the values of F_t and F_0 in equations (3) and (4) are equal to the values at $\beta = 0$, irrespective of β. Higdon and Muldowney (1995) employed a spectral boundary element method to compute F_t and F_0. For a particle near contact with the pore wall, they also used a lubrication theory to predict the limiting values, and they developed compact algebraic expressions which represent the obtained numerical data over the entire range of β for $a/r_c < 0.9$. Since their results of F_t and F_0 do not agree well with those of Sugihara-Seki (2004) for $a/r_c = 0.7$, we computed F_t and F_0 for various a/r_c in the current study.

Figure 2 shows a comparison of the present results of F_t and F_0 with those given by Higdon and Muldowney (1995) for small size ratios (see figure 2(a)) and for large size ratios (see figure 2(b)). Figure 2(a) indicates an excellent agreement of F_t and F_0 values over the whole range of β for small size ratios, while figure 2(b) shows a discrepancy between the results of Higdon and Muldowney (1995) and the present study for large size ratios at off-center positions. For comparison, the results of Sugihara-Seki (2004) are also plotted in figures 2(a) and (b) by dash-dotted lines for $a/r_c = 0.3$ and 0.7, which are almost visually indistinguishable from the corresponding curves of the present study.

As an example of the interaction energy $E(\beta)$, figure 3 shows the Boltzmann factor $\exp(-E(\beta)/kT)$ as a function of β, for $r_c = 10$ nm, $q_s = q_c = -0.01$ C/m^2, and $C_0 = 0.10$ M. This ion concentration corresponds to $\lambda_D = 0.95$ nm for aqueous solutions

at $T = 310$ K. Figure 3 indicates a sharp decrease in Boltzmann factor as the size ratio a/r_c increases. It can be also shown that the Boltzmann factor decreases with decreasing ion concentration or increasing Debye length (Akinaga *et al* 2008). For comparison, the corresponding results of Smith and Deen (1983) are plotted by thin lines, which show some discrepancy from the present results at large β. This discrepancy becomes larger for the cases of larger Debye length or larger charge densities.

In figures 4 and 5, the hindrance factors H and W are plotted as functions of the size ratio a/r_c for $r_c = 10$ nm, $q_s = -0.01$ C/m^2, $q_c = -0.01$, -0.02 C/m^2 and $C_0 = 0.01$, 0.04, 0.1, and 0.15 M. Figures 4 and 5 show that both of H and W decrease as the size ratio a/r_c is increased. The H curves are found to decrease more steeply than the W curves, as already pointed out by Dechadilok and Deen (2006) for uncharged cases. For reference, the curves of H and W in the absence of electric charge (i.e., $q_c = q_s = 0$) are plotted as thin dotted curves in figures 4 and 5. The thin dotted curves are higher than any other curves of H and W, indicating that the repulsive electrostatic interaction decreases the values of H and W or increases the hindrance effect on the diffusive and convective transport of the solute.

The dependence of H and W on the Debye length is plotted in figures 6 and 7, respectively, for $r_c = 10$ nm, $q_s = -0.01$ C/m^2, $q_c = -0.01$, -0.02 C/m^2 and $a/r_c = 0.2$, 0.4, 0.6 and 0.8. The horizontal lines represent asymptotic values corresponding to uncharged cases. Note that the Debye length represents a characteristic distance of the charge effect from the surface charge or a characteristic double-layer thickness. It is seen from figures 6 and 7 that an increase in Debye length or a decrease in ion concentration diminishes the values of H and W, which corresponds to an enlargement of the hindrance of the solute transport.

4. Discussion

In the derivation of equations (1)-(4), the effect of solute rotation on the transport coefficients is neglected, although a freely floating solute usually rotates in the flow when it is placed at off-center positions in the pore. Sugihara-Seki (2004) computed the hydrodynamic torques as well as drag forces exerted on a spherical solute when it is translating or rotating in an otherwise quiescent fluid, or it is immersed stationary in a pressure driven flow. The effect of the rotational motion on the transport coefficients was shown to be negligible compared to those by the translational motion and by the pressure driven flow. In the present study, therefore, we did not include the effect of solute rotation on H and W.

As shown in figure 2, our obtained values of F_t and F_0 are somewhat different from those given by Higdon and Muldowney (1995) for large size ratios a/r_c. For clarity, we have plotted the differences between the present results and the corresponding values given by Higdon and Muldowney (1995) in figure 8(a), for $a/r_c = 0.6$, 0.7 and 0.8. It is seen from figure 8(a) that the discrepancies are small for particles placed near the pore centerline (small β) and near contact with the pore wall (large β). The differences

between the two results at $\beta = 0$ are within 0.1 %, irrespective of the size ratio. In contrast, the differences are significant in moderate ranges of β for large size ratios as shown in figure 8(a). The maximum discrepancies are at most 1 % for $a/r_c < 0.2$, and several % for $a/r_c < 0.5$, and more than 10 % for $a/r_c > 0.8$.

Quite recently, Bhattacharya *et al* (2010) developed a method to simulate the general creeping flow involving the particle-conduit system, and determined the force on a translating spherical particle in a cylindrical pore or that on a stationary particle immersed in a pressure-driven parabolic flow. Figure 8(b) shows a comparison of the F_t or F_0 values in the present study, Higdon and Muldowney (1995) and Bhattacharya *et al* (2010), for the size ratio $a/r_c = 0.5$. As shown in figure 8(b), the dash-dotted curves given by Bhattacharya *et al* (2010) are higher than the other two curves over the whole range of β. The reason of this discrepancy, especially even at $\beta = 0$, is not apparent. As β increases from zero, the dash-dotted curves seem to approach gradually the solid curves representing the present results. To authors' knowledge, there are no further available reports which can be compared with the present results of the drag coefficients for off-axis positions.

Since Dechadilok and Deen (2006) adopted the values of F_t and F_0 of Higdon and Muldowney (1995) to estimate H and W for uncharged cases, there may be some discrepancy between the present results of H and W at $q_c = q_s = 0$ and the corresponding results of Dechadilok and Deen (2006). From a least-squares fit to the H and W values for $0 < a/r_c < 0.95$, Dechadilok and Deen (2006) provided the analytic expressions:

$$H(\lambda) = 1 + \frac{9}{8}\lambda \ln \lambda - 1.56034\lambda + 0.528155\lambda^2 + 1.91521\lambda^3 - 2.81903\lambda^4 + 0.270788\lambda^5 + 1.10115\lambda^6 - 0.435933\lambda^7, \tag{12}$$

$$W(\lambda) = (1-\lambda)\frac{1 + 3.876\lambda - 1.907\lambda^2 - 0.834\lambda^3}{1 + 1.867\lambda - 0.741\lambda^2}, \tag{13}$$

where $\lambda = a/r_c$. These curves are plotted as thin dashed curves in figures 4 and 5, respectively, for comparison. In these figures, the thin dotted curves of the present results and the corresponding thin dashed curves by Dechadilok and Deen (2006) are very close to each other, indicating that the differences in F_t and F_0 values have little effects on the hindrance factors H and W.

For charged cases, figures 4-7 indicate that the electrostatic repulsive interaction decreases the hindrance factors H and W. This effect is more significant for smaller ion concentration or larger Debye length. Even at rather large ion concentrations ($C_0 \sim 0.15$ M or $r_c/\lambda_D \sim 12.8$) corresponding to the physiological range of the blood, the H and W values are affected significantly by the electrostatic interaction between the solute and pore charge. Dechadilok and Deen (2009) reported a similar effect on H by adopting approximate expressions of $E(\beta)$. Since they are interested in the contribution of the double-layer distortion caused by particle motion to H, which is minimized for small Debye lengths (large C_0) and amplified for large Debye lengths (small C_0), the parameter values they examined are confined to rather large Debye lengths. In the present study,

in contrast, we have restricted our analyses to the cases of smaller Debye lengths, where the Debye-Hückel approximation is appropriate (Smith and Deen 1980). Accordingly, we cannot compare directly our results with those of Dechadilok and Deen (2009).

In the present study, we assumed that electric charge influences only the equilibrium distribution of solute within the pore, i.e. the interaction energy E, and neglected the charge effect on F_t or F_0 which may be caused by the distortion of the electric double layer. Dechadilok and Deen (2009) investigated the effect of the double-layer distortion on H, and concluded that the electrostatic effect on E is more important determinant of the overall diffusive permeability. Thus, inclusion of the double-layer distortion in the analysis would not change the conclusion of the present study.

In evaluating the interaction energy, we have adopted the Debye-Hückel equation, a linearized form of the Poisson-Boltzmann equation, to calculate the electrical potential. A recent study of Bhalla and Deen (2009) reported that the Boltzmann factors are nearly identical in a certain range of parameters, irrespective of whether they are derived from the Poisson-Boltzmann equation or from the Debye-Hückel equation. However, our preliminary study indicated some discrepancy between them in a similar parameter range (Akinaga and Sugihara-Seki 2011). This discrepancy will be considered in the study subsequent to this work (Akinaga et al. 2011).

5. Conclusion

We examined the electrostatic effect on the solute transport across a membrane with circular cylindrical pores, by combining numerical results of the hydrodynamic and electrostatic analyses. It was found that the electrostatic repulsive interaction between the solute and pore charge on the solute and the pore wall could enhance the hindrance of the solute transport, especially at the cases of large solute size, large charge densities and low ion concentration.

Acknowledgments

This research has been supported in part by the Grant-in-Aid for Scientific Research (B) (No. 23360087) from JSPS and the Special Research Fund, Kansai University.

References

Akinaga T, Sugihara-Seki M and Itano T 2008 Electrical charge effect on osmotic flow through pores *J. Phys. Soc. Jpn* **77** 053401-1-4

Akinaga T and Sugihara-Seki M 2011 Fluid mechanical and electrostatic study on the osmotic flow through circular cylindrical pores *Submitted to J. Biorheol.*

Akinaga T, O-tani H and Sugihara-Seki M 2011 Charge effects on hindrance factors for diffusion and convection of solute in pores II *To be submitted to Fluid Dyn. Res.*

Bhalla G and Deen WM 2009 Effects of charge on osmotic reflection coefficients of macromolecules in porous memburanes *J. Colloid Int. Sci.* **333** 363–372

Bhattacharya S, Mishara C and Bhattacharya S 2010 Analysis of general creeping motion of a sphere inside a cylinder *J. Fluid Mech.* **642** 295–328

Curry FE 1984 Mechanics and thermodynamics of transcapillary exchange *Handbook of Physiology* sec 2 vol 4 ed Renkin EM and Mickel CC (Bethesda : American Physiological Society) pp 309–374

Dechadilok P and Deen WM 2006 Hindrance factors for diffusion and convection in pores *Ind. Eng. Chem. Res.* **45** 6953–6959

Dechadilok P and Deen WM 2009 Electrostatic and electrokinetic effects on hindered diffusion in pores *J. Membrane Science* **336** 7–16

Deen WM 1987 Hindered transport of large molecules in liquid-filled pores *AIChE J.* **33** 1409–1425

Higdon JJL and Muldowney GP 1995 Resistance functions for spherical particles, droplets and bubbles in cylindrical tubes *J. Fluid Mech.* **298** 193–210

Smith FG and Deen WM 1980 Electrostatic double-layer interactions for spherical colloids in cylindrical pores *J. Colloid Int. Sci.* **78** 444–465

Smith FG and Deen WM 1983 Electrostatic effects on the partitioning of spherical colloids between dilute bulk solution and cylindrical pores *J. Colloid Int. Sci.* **91** 571–590

O-tani H and Sugihara-Seki M 2010 Two phase model analysis for the Stokes flow past a sphere attached to the circular tube wall *Nagare* **29** 363–371 (in Japanese)

Schwab Ch 1998 *p- and hp- Finite Element Methods* (Oxford : Clarendon press)

Sugihara-Seki M 2004 Motion of a sphere in a cylindrical tube filled with a Brinkman medium *Fluid Dyn. Res.* **34** 59–76

Sugihara-Seki M, Akinaga T and Itano T 2010 Effects of electric charge on osmotic flow across periodically arranged circular cylinders *J. Fluid Mech.* **664** 174–192

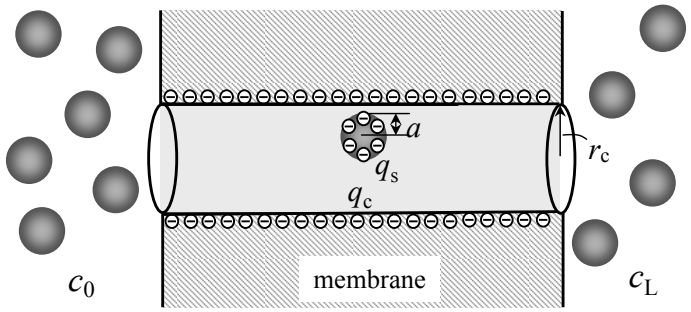

Figure 1. Sketch of the solute transport across a membrane with circular cylindrical pores of radius r_c and length L. Spherical solutes of radius a are suspended in an electrolyte solution containing small ions. The surfaces of the pore wall and solutes are electrically charged with constant densities q_c and q_s, respectively.

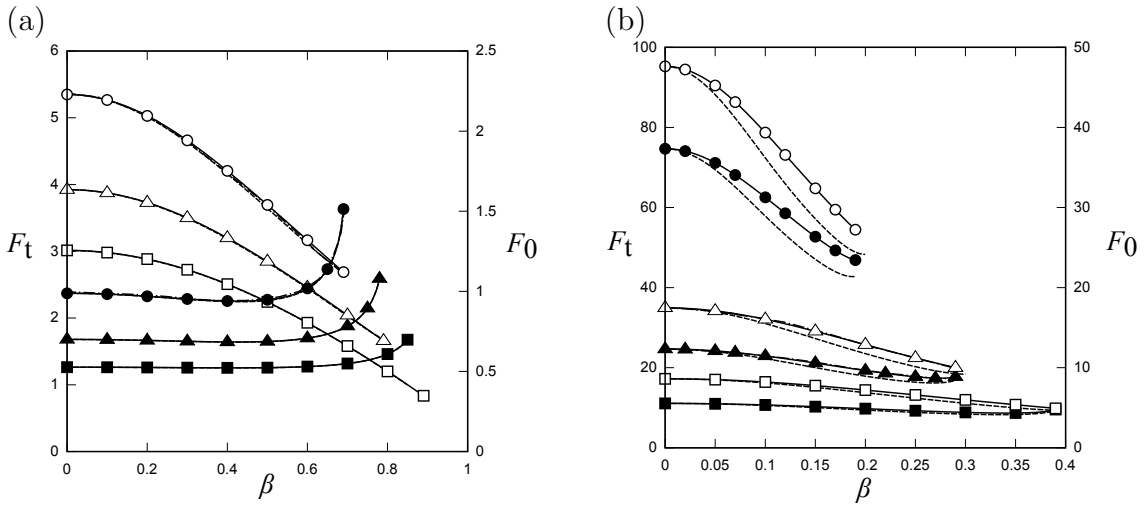

Figure 2. Drag coefficients F_t and F_0 for (a) $a/r_c = 0.2$ (rectangles), 0.3 (triangles) and 0.4 (circles) and for (b) $a/r_c = 0.6$ (rectangles), 0.7 (triangles) and 0.8 (circles). Closed symbols represent the values of F_t and open symbols represent the values of F_0. The solid lines are the present results and the dashed lines are the results obtained by Higdon and Muldowney (1995). For comparison, the results obtained by Sugihara-Seki (2004) are plotted by dash-dotted lines for $a/r_c = 0.3$ in (a) and $a/r_c = 0.7$ in (b).

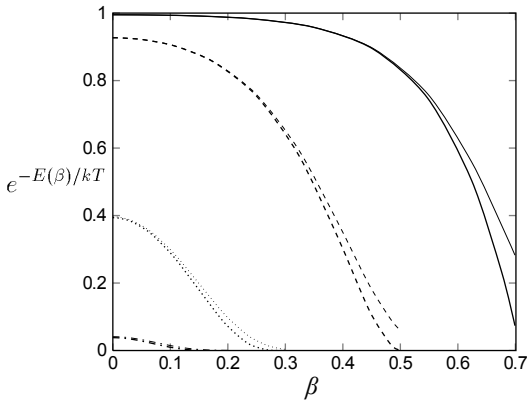

Figure 3. The Boltzmann factor $\exp(-E(\beta)/kT)$ as a function of the relative radial position of the solute center, for $r_c = 10$ nm, $q_s = q_c = -0.01$ C/m^2, $C_0 = 0.10$ M and $a/r_c = 0.3$ (solid line), 0.5 (dashed line), 0.7 (dotted line) and 0.8 (dash-dotted line). The corresponding results of Smith and Deen (1983) are plotted by thin lines, for comparison.

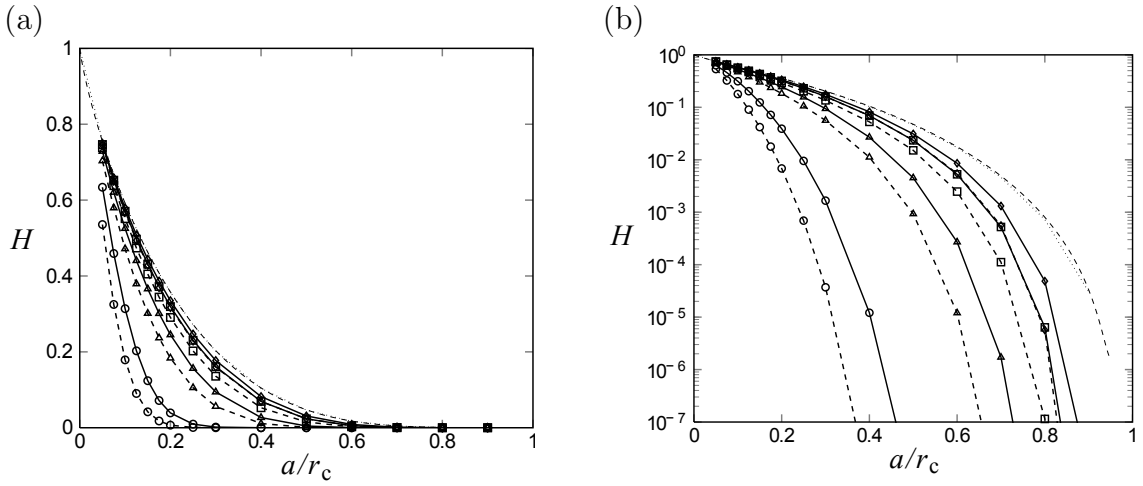

Figure 4. The hindrance factor H as a function of the size ratio a/r_c for $r_c = 10$ nm, $q_s = -0.01$ C/m^2, $q_c = -0.01$, -0.02 C/m^2 and $C_0 = 0.01$ M (circles), 0.04 M (triangles), 0.1 M (rectangles), and 0.15 M (diamonds). The solid lines represent the values for $q_c = -0.01$ C/m^2 and the dashed lines represent the values for $q_c = -0.02$ C/m^2. The results of uncharged cases are given by thin dotted line (the present result) and by thin dashed line (equation (12)).

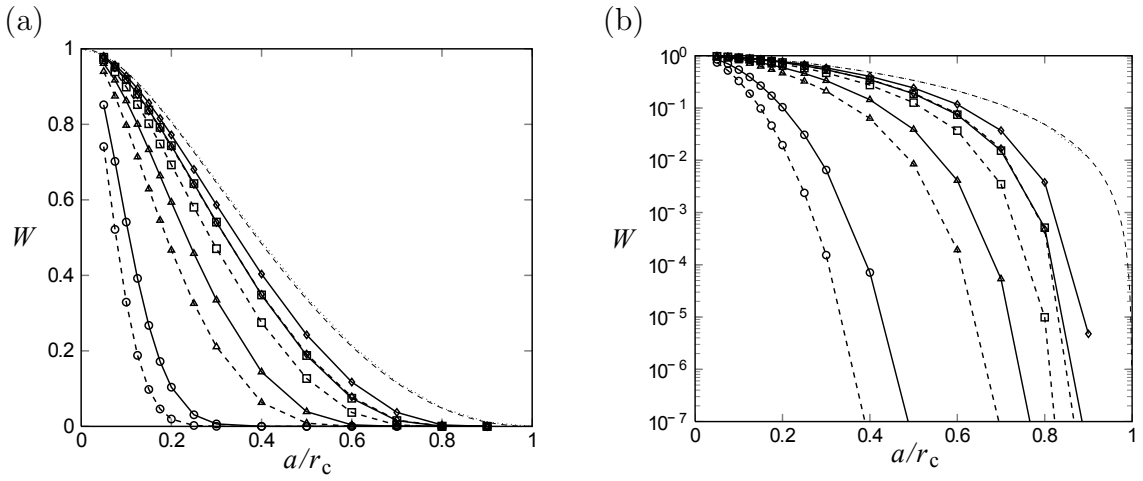

Figure 5. The hindrance factor W as a function of the size ratio a/r_c for $r_c = 10$ nm, $q_s = -0.01$ C/m^2, $q_c = -0.01$, -0.02 C/m^2 and $C_0 = 0.01$ M (circles), 0.04 M (triangles), 0.1 M (rectangles), and 0.15 M (diamonds). The solid lines represent the values for $q_c = -0.01$ C/m^2 and the dashed lines represent the values for $q_c = -0.02$ C/m^2. The results of uncharged cases are given by thin dotted line (the present result) and by thin dashed line (equation (13)).

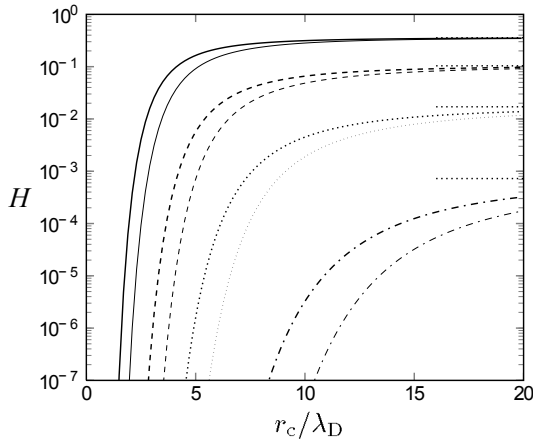

Figure 6. The hindrance factor H as a function of the ratio r_c/λ_D, for $r_c = 10$ nm, $q_s = -0.01$ C/m^2, $q_c = -0.01$, -0.02 C/m^2 and $a/r_c = 0.2$ (solid lines), 0.4 (dashed lines), 0.6 (dotted lines) and 0.8 (dash-dotted lines). The thick lines represent the values for $q_c = -0.01$ C/m^2 and the thin lines represent the values for $q_c = -0.02$ C/m^2. The horizontal lines on the right side indicate asymptotic values approached at high ion concentrations.

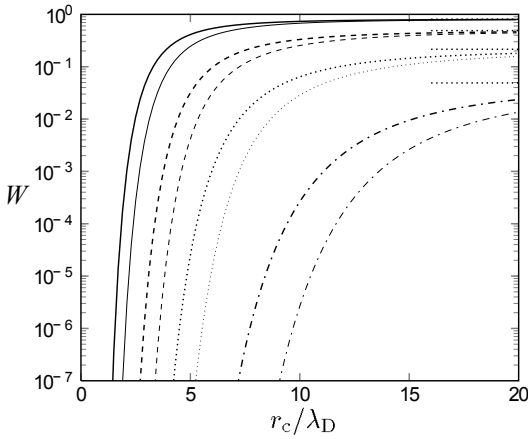

Figure 7. The hindrance factor W as a function of the ratio r_c/λ_D, for $r_c = 10$ nm, $q_s = -0.01$ C/m^2, $q_c = -0.01$, -0.02 C/m^2 and $a/r_c = 0.2$ (solid lines), 0.4 (dashed lines), 0.6 (dotted lines) and 0.8 (dash-dotted lines). The thick lines represent the values for $q_c = -0.01$ C/m^2 and the thin lines represent the values for $q_c = -0.02$ C/m^2. The horizontal lines on the right side indicate asymptotic values approached at high ion concentrations.

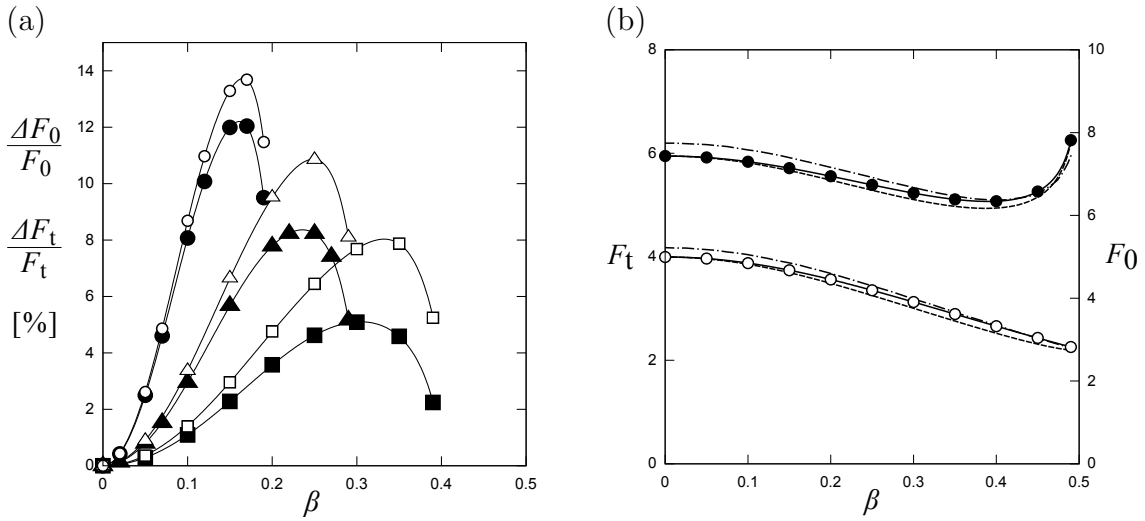

Figure 8. (a) Differences of the drag coefficients between the present study and Higdon and Muldowney (1995) compared to the present results, $\Delta F_t/F_t$ and $\Delta F_0/F_0$, for the size ratios $a/r_c = 0.6$ (rectangles), 0.7 (triangles) and 0.8 (circles). The solid symbols represent $\Delta F_t/F_t$ and the open symbols represent $\Delta F_0/F_0$. (b) The drag coefficients F_t and F_0 for $a/r_c = 0.5$ as functions of the relative radial position of the solute center. The solid and open circles represent the F_t and F_0 values of the present study, respectively. The dashed lines denote the corresponding values obtained by Higdon and Muldowney (1995), and dash-dotted lines by Bhattacharya *et al* (2010).